



## Radiation and structural defects in $\text{YVO}_4$ : Nd laser crystals

ŚLAWOMIR M. KACZMAREK<sup>A</sup>, RYSZARD JABŁOŃSKI<sup>B</sup>,  
MAREK ŚWIRKOWICZ<sup>B</sup>, WOJCIECH PASZKOWICZ<sup>C</sup>

<sup>A</sup> Institute of Optoelectronics MUT, 2 Kaliski Str., 00-908 Warsaw Poland

<sup>B</sup> Institute of Electronic Materials Technology, 133 Wólczyńska Str., 01-919  
Warsaw, Poland

<sup>C</sup> Institute of Physics PAS, 32/46 Al. Lotników, 02-668 Warsaw, Poland

**Abstract:** Optical properties of  $\text{YVO}_4$  and  $\text{YVO}_4$ :Nd crystals before and after ionizing radiation treatment with gamma quanta and electrons were presented. The obtained  $\text{YVO}_4$  and  $\text{YVO}_4$ :Nd (1 at. % Nd) single crystals show lower content of point defects (growth defects, e.g. oxygen vacancies) and consequently, lower susceptibility to ionizing radiation than YAG: Nd crystals.

Radioluminescence spectra show dumping of Nd emission in Nd doped  $\text{YVO}_4$  single crystal. The presence of  $\text{V}^{4+}$  ions and  $\text{Gd}^{3+}$  (unintentional dopant) in  $\text{YVO}_4$  at  $\text{V}^{5+}$  sites (compensated by oxide vacancies) and  $\text{Y}^{3+}$  sites, respectively, is found from electron spin resonance measurements. Moreover, the angular dependence of resonance line position of electron spin resonance may indicate that unrecognised structural defect is associated with cation sites occupied by Nd ions.

Annealing experiments in nitrogen and hydrogen were performed. The nitrogen atmosphere has a little influence on the  $\text{YVO}_4$  crystals while a  $\text{YVO}_4$ :Nd crystal annealed in hydrogen at 1200°C for 1h underwent a phase transition to  $\text{YVO}_3$ . The refined lattice parameters obtained for the latter case,  $a_0=5.2858(1)$  Å,  $b_0=5.5956(2)$  Å and  $c_0=7.5854(2)$  Å, are slightly larger only than those of  $\text{YVO}_3$ .

**Keywords:** absorption, electron spin resonance, gamma and electron irradiations

**UKD symbols:** 548.14

## 1. INTRODUCTION

Yttrium orthovanadate single crystals  $\text{YVO}_4$  doped with rare earth elements are very attractive laser material currently used for microlaser and diode laser pumped solid -state lasers. Physical properties make them superior to neodymium doped YAG [1].

In comparison with YAG: Nd (for diode laser pumping), Nd:YVO<sub>4</sub> lasers reveal the advantages of lower dependence of pump wavelength on temperature, high slope efficiency, lower lasing threshold, linearly polarised emission and tendency to the single-mode output. The peak pump wavelength for these two crystals is 808 nm, the standard wavelength of currently manufactured high power diodes for laser pumping. For the applications in which compact design and single longitudinal-mode output is needed YVO<sub>4</sub>: Nd shows its particular advantages over other laser crystals actually used [2, 3].

YVO<sub>4</sub>: Nd crystals show high absorption coefficient, high optical transparency in the 400-5000 nm range, large stimulated emission cross section at lasing wavelength ( $25 \cdot 10^{-19} \text{cm}^2$ ). Lasing wavelengths are 1,064  $\mu\text{m}$  and 1,342  $\mu\text{m}$ . Fluorescent life time is 90  $\mu\text{s}$ , diode pumped optical to optical efficiency exceeds 60%. Strong birefringence ( $n_o=1.958$ ,  $n_e=2.168$  at 1064 nm), good optical, physical and mechanical properties (crystal: structure – tetragonal:  $a = 7,12 \text{ \AA}$ ;  $c = 6,29 \text{ \AA}$ ). Density: 4,22  $\text{g/cm}^3$ . Mohs hardness  $\sim 5$ . Thermal expansion coefficient:  $\alpha_a = 4,43 \cdot 10^{-6}/\text{K}$ . Thermal conductivity coefficient:  $\parallel c$ ,  $\beta = 0,0523 \text{ Wcm/K}$ ,  $\perp c$ ,  $\beta = 0,0510 \text{ Wcm/K}$ ) [3].

For practical exploitation of the above mentioned properties, scattering free Nd:YVO<sub>4</sub> single crystals of high quality are required. Since the scattering is related to defect structure of the crystal, special attention must be paid to the growth conditions. Compositional variations in YVO<sub>4</sub> crystal have been suggested based on variations in optical properties [4], the solidification behaviour [5] and the annealing behaviour [6] of YVO<sub>4</sub>.

The main goal of the paper was to study some kinds of point and structural defects as well as selected optical properties of YVO<sub>4</sub>: Nd single crystals.

## 2. EXPERIMENTAL SETUP

YVO<sub>4</sub> and Nd:YVO<sub>4</sub> crystals were grown by Czochralski method with use of induction heating from stoichiometric mixture of Y<sub>2</sub>O<sub>3</sub> and V<sub>2</sub>O<sub>2</sub> oxides. The nominal Nd<sup>3+</sup> concentration of the Nd doped samples was 1 at. %. Details of the growth conditions have been presented elsewhere [7].

The samples were prepared by cutting and polishing (approximate dimensions 10 mm in length and 1 mm in thickness). After measurement of the transmission,

the absorption,  $K$  and then, after a treatment, the value,  $\Delta K$ , was calculated according to the formula:

$$\Delta K(\lambda) = 1/d \ln ( T_1(\lambda)/T_2(\lambda) ) \quad (1)$$

where  $\lambda$  is the wavelength,  $d$  is the sample thickness,  $T_1$  and  $T_2$  are the transmissions of the sample before and after an appropriate treatment procedure, respectively. Absorption spectra were taken at a temperature of 300 K in the spectral range 190-7000 nm using Perkin-Elmer spectrophotometer (190-1100 nm) and a FTIR spectrometer (1400-25000 nm) before and after gamma irradiation. Luminescence spectrum was measured at a temperature of 300 K in the spectral range 400-1200 nm with use of third harmonics of YAG: Nd crystal ( $\lambda_{\text{ex}}=355$  nm).

The samples were irradiated by gamma photons immediately after the crystal growth process. The gamma source of <sup>60</sup>Co with an efficiency of 1.5 Gy/sec was used. The gamma doses applied were up to 10<sup>6</sup> Gy. The samples for ESR investigations were irradiated also by electrons with fluencies 10<sup>14</sup> - 5 x 10<sup>16</sup> electrons/cm<sup>2</sup> at 77K. Electron irradiations at an energy of 1MeV were performed using a Van de Graaf accelerator.

The dimensions of samples for ESR investigation were the following 3.5x3.5x2 mm. They were investigated using a Bruker ESP300 ESR spectrometer (X-band). The spectrometer was equipped with helium flow cryostat type ESR900 Oxford Instruments. The ESR investigations were performed in the temperature range from 4 to 35 K and microwave power from 0.002 to 200 mW.

Radioluminescence spectra were measured in the range 200-850 nm using excitation with X-rays (DRON, 35 kV / 25 mA) and Spectrograph: ARC SpectraPro-500i (Hol-UV 1200 gr/mm grating and 500 nm blazed grating 1200 gr/mm, 0.5 mm slits), PMT: Hamamatsu R928 (1000 V).

X-ray diffraction measurement was performed for YVO<sub>3</sub>:Nd (obtained by annealing of YVO<sub>4</sub>:Nd in hydrogen) using an automated Bragg-Brentano diffractometer working in the step-scanning mode and equipped with a scintillation counter, applying Ni-filtered CuK $\alpha$  radiation. To minimize the effect of preferred orientation on peak intensities, the crystal was finely ground and the obtained powder was loosely dusted on a specimen holder covered with a thin layer of vaseline. A low-background single-crystalline-quartz specimen holder supplied by GEM-DUGOUT was applied. Before the analysis, the background was subtracted and the K $\alpha_2$  component was stripped using the Rachinger method. A freeware program (DHN-PDS) was used for these operations. Peak positions were determined using a profile-fitting routine. Refinement of unit-cell dimensions was performed using an unweighted least-squares method.

### 3. RESULTS AND DISCUSSION

#### 3.1 Absorption and luminescence measurements

Figs 1 presents absorption spectrum of Nd doped YVO<sub>4</sub> single crystal for the all transitions from <sup>4</sup>I<sub>9/2</sub> manifold (ground state) in range 200-800 nm in comparison with Nd doped YAG. As seen fundamental absorption edge (FAE) is about 340 nm. The ratio of the absorption's of YVO<sub>4</sub>:Nd with respect to YAG: Nd for λ=808 nm is as high as 4. An increase of absorption with a decrease of wavelength which is seen for small wavelengths is connected rather with accuracy of surface polishing of the investigated samples.

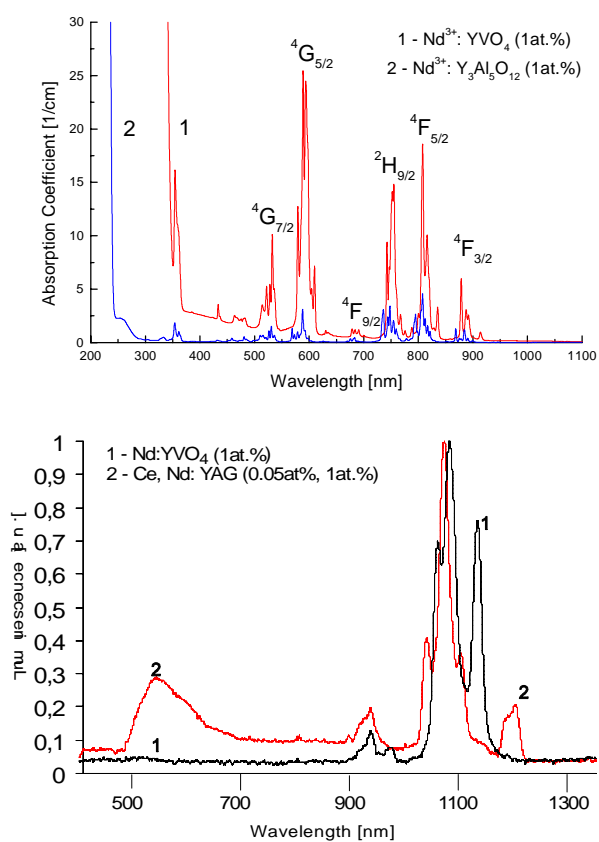


Fig. 1. Absorption of YVO<sub>4</sub>: Nd (1 at. % Nd) single crystal in comparison with YAG:Nd (1 at. % Nd)

Fig. 2. <sup>4</sup>F<sub>3/2</sub> → <sup>4</sup>I<sub>11/2</sub> (near 1100 nm) and <sup>4</sup>F<sub>3/2</sub> → <sup>4</sup>I<sub>9/2</sub> (near 940 nm) photoluminescence spectra of Nd<sup>3+</sup> for (1) YVO<sub>4</sub>:Nd and YAG: Ce, Nd (0.05 at. % Ce, 1 at. % Nd) and 5d-4f emission of Ce<sup>3+</sup> in YAG: Ce, Nd at 300 K

Fig. 2 shows luminescence spectrum of  $\text{YVO}_4:\text{Nd}$  in comparison with YAG:Ce, Nd both after gamma irradiation with a dose of  $10^6$  Gy. Some changes are observed in relative intensities of photoluminescence with respect to non-irradiated crystal [8]. They are probably attributed to a change in defect structure of  $\text{YVO}_4:\text{Nd}$  single crystal after gamma irradiation.

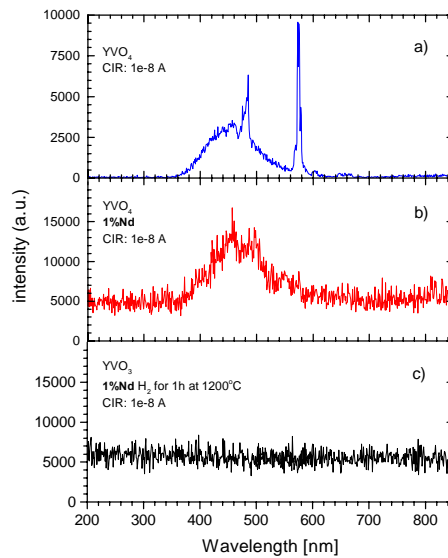


Fig. 3. Radioluminescence spectrum of (a)  $\text{YVO}_4$ , (b)  $\text{YVO}_4:\text{Nd}$  (1 at. % Nd), and (c)  $\text{YVO}_4:\text{Nd}$  (1 at. % Nd) after annealing in hydrogen atmosphere at  $1200^\circ\text{C}$  for 1 h

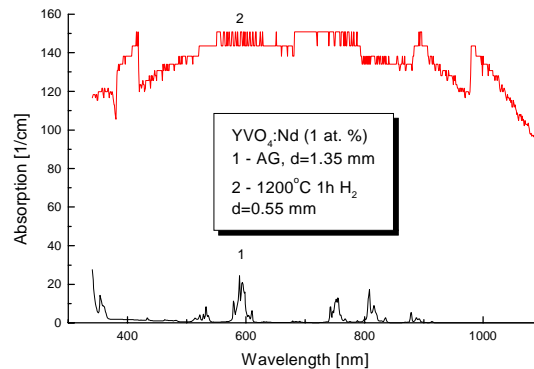


Fig. 4. Absorption of (1)  $\text{YVO}_4:\text{Nd}^{3+}$  single crystal and (2) annealed in hydrogen at  $1200^\circ\text{C}$  for 1 h

More accurate analysis of the photoluminescence features in the short wave range may be obtained using radioluminescence studies. Fig. 3 shows radioluminescence measurements of pure  $\text{YVO}_4$  single crystal (a),  $\text{YVO}_4:\text{Nd}$  single crystal (b) and  $\text{YVO}_3:\text{Nd}$  crystal (c). As seen fundamental absorption edge is described as previously for absorption measurements (340 nm) and besides a band picked at 460 nm (probably excitonic origin) some non-controlled impurities are seen at 485 and 575 nm for pure  $\text{YVO}_4$  crystal, while for  $\text{YVO}_4:\text{Nd}$  crystals all the emissions are thought to be damped by Nd ions, which do not give any self-emission. This may be due to a structural defect in Nd positions. From the above it seems, that  $\text{YVO}_4:\text{Nd}$  crystals are more defected than  $\text{YVO}_4$ .

The above radioluminescence characteristics was obtained for current input range equal to  $10^{-8}$  A for  $\text{YVO}_4$ ,  $\text{YVO}_4:\text{Nd}$  and  $\text{YVO}_3:\text{Nd}$  crystals.

### 3.2 X-ray powder diffraction

From Fig. 3c it result that after annealing of the Nd:  $\text{YVO}_4$  crystal in hydrogen a band picked at about 460 nm vanishes. Moreover, annealing in hydrogen atmosphere causes a phase transition from  $\text{YVO}_4:\text{Nd}$  crystals to  $\text{YVO}_3:\text{Nd}$ . The resulting  $\text{YVO}_3:\text{Nd}$  crystal is almost not transparent (black in color) in UV-VIS range (absorption of the crystals increases to about  $100\text{ cm}^{-1}$  – see Fig. 4).

X-ray powder diffraction pattern for the studied sample is shown in Fig. 5.

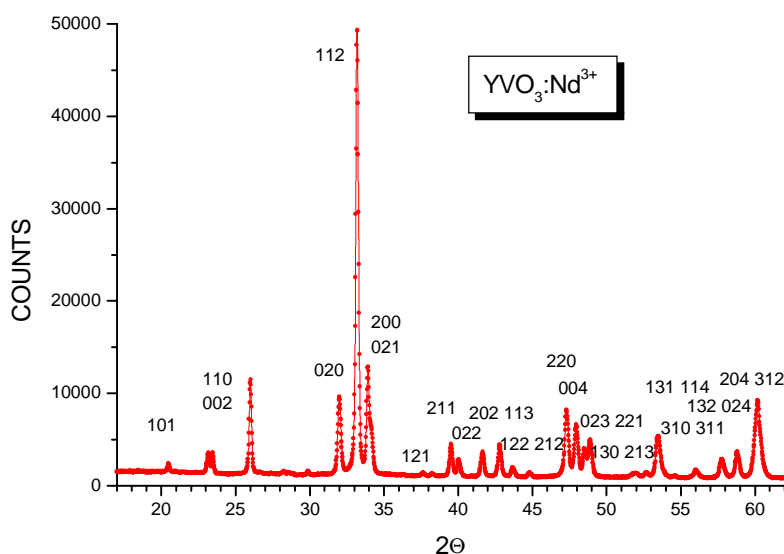


Fig. 5. Raw powder diffraction pattern of  $\text{YVO}_3:\text{Nd}$  obtained by annealing of  $\text{YVO}_4:\text{Nd}$  in hydrogen at  $1200^\circ\text{C}$  for 1 hour.

The phase analysis shows that the crystal is a single phase perovskite, space group Pbnm (62) known in the RVO<sub>3</sub> compound series. The refined lattice parameters obtained from refinement of 29 reflections in the range 20-85 degrees 2 $\Theta$ ,  $a_0 = 5.2858$  (1) Å,  $b_0 = 5.5956$  (2) Å,  $c_0 = 7.5854$  (2) Å, are slightly larger than those of YVO<sub>3</sub> ( $a_0 = 5.274$  Å,  $b_0 = 5.590$  Å and  $c_0 = 7.574$  Å [9].) The difference may be at least partially attributed to the presence of Nd ions at Y sites.

### 3.3 Additional absorption after gamma irradiation

Fig. 6 shows additional absorption for YVO<sub>4</sub> and YVO<sub>4</sub>:Nd single crystals after gamma irradiation with a dose of 10<sup>5</sup> Gy in comparison with YAG' s. The YVO<sub>4</sub> single crystal is found to be less susceptible to gamma irradiation than YAG (maximum of additional absorption for YVO<sub>4</sub> crystal has a value of about 0.25 cm<sup>-1</sup> while for YAG crystal this value is equal to about 1 cm<sup>-1</sup>). Moreover, in the additional absorption spectrum the presence of Fe ions absorption (256 nm and 310 nm for YAG and YAG: Nd crystals) and F-centre absorption (400-450 nm for YAG and YAG: Nd crystals) is not observed.

After gamma irradiation of YVO<sub>4</sub> and YVO<sub>4</sub>:Nd crystals two bands arise in absorption spectrum with maxima at: 380 and 556 nm (Fig. 6). They are comparable with additional absorption of YAG' s but their intensity is much lower.

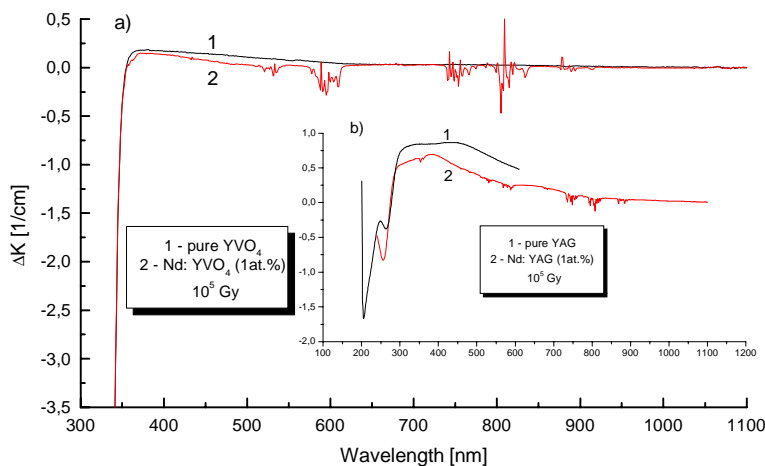


Fig. 6. Additional absorption after gamma irradiation with a dose of 10<sup>5</sup> Gy in YVO<sub>4</sub> and Nd:YVO<sub>4</sub> single crystals in comparison with YAG one

In summary, in YVO<sub>4</sub> crystal the density of point defects is lower than in YAG; the YVO<sub>4</sub> crystal shows absence of non-controlled impurity (optically active) absorption.

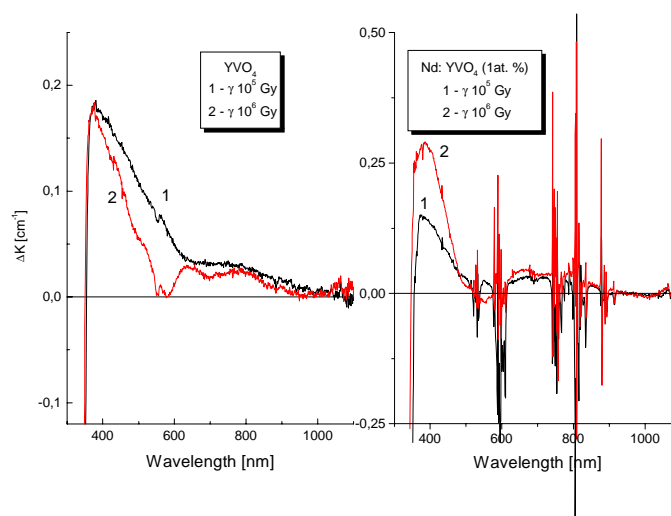


Fig. 7. Additional absorption in  $\text{YVO}_4$  and  $\text{YVO}_4:\text{Nd}$  crystals after gamma irradiation with doses: 1 –  $10^5$  Gy and 2 –  $10^6$  Gy

Irradiations with gamma rays performed with greater doses ( $10^6$  Gy) show that further increase in absorption value is not observed for pure  $\text{YVO}_4$  crystals. For Nd doped  $\text{YVO}_4$  crystals, doubling of intensity of additional absorption after gamma irradiation with a dose of  $10^6$  Gy with respect to  $10^5$  Gy is seen (see Fig. 7). Therefore, saturation may be concluded for doses as high as  $10^5$  Gy applied to  $\text{YVO}_4$  single crystal (all point defects undergo recharging process), while for  $\text{YVO}_4:\text{Nd}$  such phenomenon does not take place (more defected structure of  $\text{YVO}_4:\text{Nd}$  single crystal). Narrow intensive lines observed in Fig. 7 for additional absorption in Nd:  $\text{YVO}_4$  crystal arise due to presence of narrow intensive Nd lines in absorption spectrum of the crystal. Small shift of absorption lines in the wavelength scale gives such large values of additional absorption.

### 3.4 ESR measurements

The  $\text{Nd}^{3+}$  ion substitutes for  $\text{Y}^{3+}$  in  $\text{YVO}_4$  single crystal. The 3+ charge state of Nd has a  $f^3$  configuration. The ground term is  ${}^4\text{I}$  and spin orbit interaction splits this term into manifolds  $J=9/2$  (the ground state) and  $11/2$ ,  $13/2$  and  $15/2$ .

The  $\text{Nd}^{3+}$  ion occupies a site of  $\text{D}_{2d}$  symmetry. The nearest neighbors to the  $\text{Nd}^{3+}$  ion are eight  $\text{O}^{2-}$  ions, which form a tetragonally distorted octahedron with the distortion axis (z) corresponding to the c axis of the crystal [8]. In the case of Nd:  $\text{YVO}_4$  single crystal, for magnetic field parallel to (001) plane, isotropic ESR spectrum with two groups of eight hyperfine lines (hfs) and one single strong line with  $I=0$  was observed.



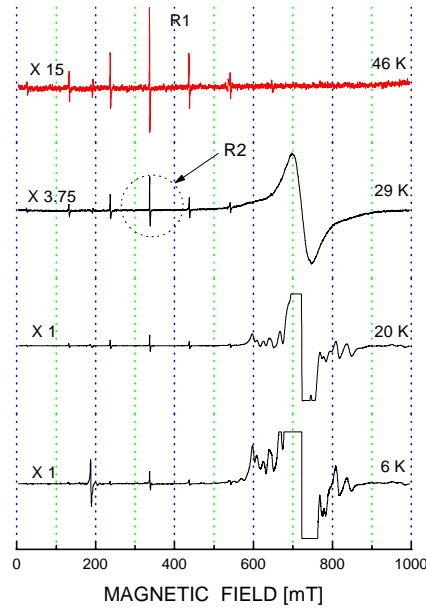


Fig. 8. Typical ESR spectrum of Nd: YVO<sub>4</sub> single crystal for H||c and different temperatures

The spectrum is described by the following spin-Hamiltonian:

$$H = g_{\parallel} \cdot \beta \cdot \mathbf{H}_z \cdot \mathbf{S}_z + g_{\perp} \cdot \beta \cdot (\mathbf{H}_x \cdot \mathbf{S}_x + \mathbf{H}_y \cdot \mathbf{S}_y) + A_{\parallel} \cdot \mathbf{I}_z \cdot \mathbf{S}_z + A_{\perp} \cdot (\mathbf{I}_x \cdot \mathbf{S}_x + \mathbf{I}_y \cdot \mathbf{S}_y) \quad (2)$$

where:  $H_x$ ,  $H_y$  – components of magnetic field,  $S=1/2$  – electron spin,  $I=0$  for even-mass isotopes and  $I=7/2$  for  $^{143}\text{Nd}$  and  $^{145}\text{Nd}$  – nucleus spin.  $A_{\parallel}$  and  $A_{\perp}$  are hfs constants,  $g$  – Lande factor and  $\beta$  is the Bohr magneton.

The calculations give  $g_{\parallel}=0.9132$ ,  $g_{\perp}=2.350(1)$ ,  $^{143}A_{\perp}=216 \cdot 10^{-4} \text{ cm}^{-1}$ ,  $^{145}A_{\perp}=138 \cdot 10^{-4} \text{ cm}^{-1}$ .  $A_{\parallel}$  was not determined because the linewidth of each hfs was very wide for this direction.

The Nd line in ESR spectrum for different temperatures is presented in Fig. 8. The ESR spectrum intensity decreases with rising temperature. Above 30K, each hfs broadens such that the resolved components are undetectable. ESR spectrum disappears completely above 45 K as a consequence of rapid spin-lattice relaxation. Moreover, in the whole measurement range from 4 K to 300 K, the anisotropy spectrum composed of seven lines with intensity distribution of about 1:3:6:10:6:3:1 is observed. It is designed as R1 and may be connected with  $\text{Gd}^{3+}$  ions in  $\text{Y}^{3+}$  sites. We found that ratio of  $\text{Gd}^{3+}$  to  $\text{Nd}^{3+}$  ions is as high as 0.0005. Additionally inside this spectrum (R2), eight-line hyperfine pattern is observed with a splitting of about 122 Gs which is (probably) a result of interaction with the

$V^{4+}$  nucleus ( $I=7/2$ , abundance=100%). After heat treatment in air at a temperature of about 1000 °C for 5 h this spectrum disappears completely. Possible explanation is that in the investigated crystal some  $V^{4+}$  ions are placed at  $V^{5+}$  positions, which are compensated by oxide vacancies. From our investigations result that the concentration of  $V^{4+}$  ions is at last two orders of magnitude lower than that of  $Nd^{3+}$  ions.

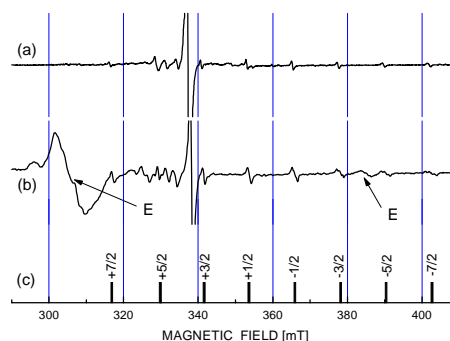


Fig. 9. ESR spectrum of  $YVO_4:V^{4+}$ ,  $H \parallel [001]$ . a) as-grown crystal,  $T=27K$ , b) electron irradiated (E),  $T=56K$ , c) predicted super hyper fine structure (shfs) of line position for  $A_c = 12.3$  mT

As seen this spectrum shows the presence of hfs structure (see also Fig. 9c).

A very interesting ESR signal is observed after ionizing radiation treatment. Irradiation with electrons leads to arising of paramagnetic defect, marked as E (on the left hand side of Fig. 9b). The only differences between effects of electron and gamma irradiations are additional ESR lines for electrons (seen on the right hand side of Fig. 9b), which can be connected with Frenkel defects. For gamma irradiated crystals, the above mentioned defect influences the ESR spectrum even for a dose as low as  $10^3$  Gy. We observed that an increase in the dose value of gamma or electron irradiation leads to arising of a paramagnetic defect in higher temperatures.

From the angular dependence in Fig. 10 result, that some defective structure exists in  $YVO_4:Nd$  single crystals. The single central ESR line ( $I=0$ ) splits close to  $[001]$  direction (compare  $H \parallel c$  and  $H \perp c$  orientations). It may be due to an existence of twins in the specimen, but not only. Broadening of  $Gd^{3+}$  lines suggest an existence also mosaic structure in the crystal. These may be a reason for which  $Nd^{3+}$  ions emission damping is observed in radioluminescence spectrum.

The non-controlled impurities observed in radioluminescence spectrum (Fig. 3) are probably  $V^{4+}$  and  $Gd^{3+}$  ions occupying  $V^{5+}$  and  $Y^{3+}$  sites, respectively. The  $V^{4+}$  ions are seen in ESR spectrum for “as grown” crystals and, after gamma or electron irradiation the amount of such ions increases. Similar phenomenon, but for vanadium doped YAG single crystals (change in a valency of V ions located at

lattice sites), has been observed in [11]. The presence of  $\text{V}^{4+}$  ions can be explained within the vanadium vacancy model for solid solution [12]. This model assumes also the presence of vanadium and oxygen vacancies being necessary for the charge compensation.

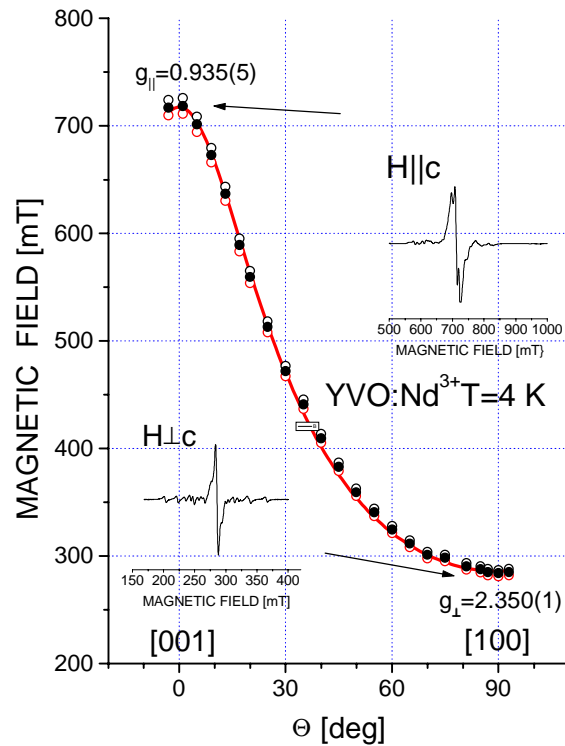


Fig. 10. Angular dependence of ESR lines of  $\text{YVO}_4:\text{Nd}$  at 4 K with magnetic field in (010) plane, circles – experimental data, solid lines - fitted theoretical curve. ESR spectra for  $H\parallel c$  and  $H\perp c$  are also seen as small figures

Annealing of  $\text{YVO}_4:\text{Nd}$  single crystal in hydrogen does not dramatically change EPR spectra. The only change found after annealing is that it shows a greater conductance, attributable to Nd atoms created after annealing onto the crystal surface.

#### 4. CONCLUSIONS

Obtained in the Institute of Electronic Materials Technology  $\text{YVO}_4$  and Nd doped  $\text{YVO}_4$  single crystals exhibit good optical quality and strong absorption in

the range of diode laser pumping (about  $19 \text{ cm}^{-1}$  in the range 750-850 nm). They had got also small amount of non-controlled impurities, e.g.  $\text{Gd}^{3+}$ , without the presence of Fe ions (as compare to YAG crystals) and small amount of growth defects, such as oxygen vacancies and solid solution ( $\text{V}^{4+}$  ions).

These crystals showed lower susceptibility to gamma and electron irradiations in comparison with YAG's. After irradiation treatment, a paramagnetic defect appears in the crystals. From the angular dependence of resonance line position of electron spin resonance result, that they may be  $\text{V}^{4+}$  ions at  $\text{V}^{5+}$  sites. The concentration of  $\text{V}^{4+}$  ions is at last two orders of magnitude lower than that of  $\text{Nd}^{3+}$  ions.

From radioluminescence (the emission of Nd ions is missing after X-ray excitation), additional absorption after  $\gamma$ -irradiation (increase in additional absorption of Nd: YAG crystal with a dose over  $10^5$  Gy is observed) and ESR measurements (Fig. 10) result that there arises some structural defect in  $\text{YVO}_4:\text{Nd}$  single crystal near Nd lattice positions resulting in emission damping of Nd ions. It may be due to the presence of twins and/or mosaic structure.

Annealing in hydrogen atmosphere at  $1200^\circ\text{C}$  of  $\text{YVO}_4:\text{Nd}$  for 1h results in phase transition to  $\text{YVO}_3:\text{Nd}$ . The question arises: is the crystal of single crystal or no. Due to necessity of long time experiments leading to the solving of above problem the answer is still open. The obtained  $\text{YVO}_3:\text{Nd}$  crystal is black and almost not transparent in UV-VIS range of absorption spectrum. Obtained by the Czochralski method  $\text{YVO}_3$  single crystals are also black in color.

Similar results were obtained earlier for magnesium orthovanadate single crystals [13]. A single crystal of orthorhombic  $\text{Mg}_3(\text{VO}_4)_2$  was transformed into cubic  $\text{Mg}_3(\text{VO}_3)_2$  at  $560^\circ\text{C}$  in 7%  $\text{H}_2$  in  $\text{N}_2$ . Colorless or slightly yellow crystals became black.

## ACKNOWLEDGMENTS

Authors deeply acknowledge Prof. T. Łukasiewicz (Institute of Electronic Materials Technology) for the supply of the present studies in the  $\text{YVO}_4$  and  $\text{YVO}_4:\text{Nd}$  crystal samples and W. Drozdowski (Institute of Physics, Nicolae Copernicus University) for radioluminescence measurements.

## REFERENCES

1. S. Erdei et al., *J. of Cryst. Growth* 172 (1997) 466-472
2. K. Chow and H.G. Knight, *Mat. Res. Bull.* 8 (1973) 1343-1350
3. S. Erdei et al., *Cryst. Res. Technol.*, 29 (1994) 815-828
4. R.C. Ropp, *J. Electrochem. Soc.*, 115 (1968) 941
5. S. Erdei and F.W. Ainger, *J. Crystal Growth* 128 (1993) 1025
6. Y. Nobe, H. Takashimata and T. Katsumata, *Optics Lett.* 19 (1994) 123

7. S.M. Kaczmarek, T. Łukasiewicz, W. Giersz, R. Jabłoński, J.K. Jabczyński, M. Świrkowicz, Z. Gałązka, W. Drozdowski, M. Kwaśny, "Growth and optical properties of Nd:YVO<sub>4</sub> laser crystals", *Proc. SPIE*, vol. **3724**, (1999), 324-328; See also: *Opto-electr. Rev.*, 7(2) (1999) 149-152
8. F.G. Anderson, P.L. Summers, H. Weidner, P. Hong, and R. E. Peale: "Interpretative crystal-field parameters: Application to Nd<sup>3+</sup> in GdVO<sub>4</sub> and YVO<sub>4</sub>", *Phys. Rev.*, B50 (20) (1994) 14802-14808
9. B.C. Chakoumakos, M.M. Abraham, L.A. Boatner, "Crystal structure refinements of zircon-type MVO<sub>4</sub> (M=Sc, Y, Ce, Pr, Nd, Tb, Ho, Er, Tm, Yb, Lu)" *J.Solid State Chemistry* **109**, 197-202 (1994)
10. R. Jabłoński, S.M. Kaczmarek, M. Świrkowicz, T. Łukasiewicz, "Electron Spin Resonance and Optical measurements of Yttrium Ortho-Vanadate, Doped with Nd<sup>3+</sup> ions", *J. of Alloys and Comp.*, in the print
11. R. Jabłoński, S.M. Kaczmarek, "Electron Spin Resonance and Optical measurements in YAG:V<sup>3+</sup> crystals", *Proc. SPIE*, vol. **3724** (1999), 346-352
12. T. Katsumata, H. Takashima, T. Michino and Y. Nobe, "Non-stoichiometry in yttrium ortho-vanadate", *Mat. Res. Bull.*, vol. 29, No. 12, (1994) 1247-1254
13. X. Wang, H. Zhang, W. Sinkler, K.R. Poeppelmeier, L.D. Marks, "Reduction of magnesium orthovanadate Mg<sub>3</sub>(VO<sub>4</sub>)<sub>2</sub>, *J. All. & Comp.*, 270 (1998) 88-94

## Defekty radiacyjne w monokryształach laserowych YVO<sub>4</sub>:Nd

**Streszczenie:** Zbadano właściwości optyczne monokryształów YVO<sub>4</sub>, YVO<sub>4</sub>:Nd oraz YVO<sub>3</sub>:Nd przed i po naświetleniu promieniowaniem gamma i elektronami. Badane monokryształy YVO<sub>4</sub>: Nd (1at.% Nd) wykazały obecność mniejszej ilości defektów punktowych i w konsekwencji mniejszą czułość na uszkodzenia radiacyjne od monokryształów YAG: Nd. Pomiar ESR wykazały obecność w tych kryształach jonów V<sup>4+</sup> w położeniach międzywęzłowych, jonów Gd<sup>3+</sup> w położeniach Y<sup>3+</sup> oraz defektu strukturalnego w otoczeniu jonu neodymu. Ten ostatni defekt jest prawdopodobnie przyczyną braku emisji jonów Nd po ich wzbudzeniu promieniowaniem X. Wygrzanie monokryształu YVO<sub>4</sub>:Nd w wodrze w temperaturze 1200°C przez 1 godzinę prowadzi do powstania nowej fazy krystalicznej, YVO<sub>3</sub>: Nd.